The Genomic Landscape of the Somatic Linker Histone Subtypes H1.1 to H1.5 in Human Cells

Annalisa Izzo, Kinga Kamieniarz-Gdula, Fidel Ramirez, Nighat Noureen, Jop Kind, Thomas Manke, Bas van Steensel, Robert Schneider

Cell Reports
Resource

The Genomic Landscape of the Somatic Linker Histone Subtypes H1.1 to H1.5 in Human Cells

Annalisa Izzo,[1,2,5] Kinga Kamieniarz-Gdula,[2,3,5] Fidel Ramírez,[2] Nighat Noureen,[2] Jop Kind,[4] Thomas Manke,[2] Bas van Steensel,[4] and Robert Schneider[1,*]
[1]Institut de Génétique et de Biologie Moléculaire et Cellulaire, CNRS UMR 7104, INSERM U 964, Université de Strasbourg, 67404 Illkirch, France
[2]Max Planck Institute of Immunobiology and Epigenetics, Stübeweg 51, 79108 Freiburg, Germany
[3]Sir William Dunn School of Pathology, University of Oxford, South Parks Road, Oxford OX1 3RE, UK
[4]Division of Gene Regulation, The Netherlands Cancer Institute, Plesmanlaan 121, 1066 CX Amsterdam, The Netherlands
[5]These authors contributed equally to this work
*Correspondence: schneidr@igbmc.fr
http://dx.doi.org/10.1016/j.celrep.2013.05.003

SUMMARY

Human cells contain five canonical, replication-dependent somatic histone H1 subtypes (H1.1, H1.2, H1.3, H1.4, and H1.5). Although they are key chromatin components, the genomic distribution of the H1 subtypes is still unknown, and their role in chromatin processes has thus far remained elusive. Here, we map the genomic localization of all somatic replication-dependent H1 subtypes in human lung fibroblasts using an integrative DNA adenine methyltransferase identification (DamID) analysis. We find in general that H1.2 to H1.5 are depleted from CpG-dense regions and active regulatory regions. H1.1 shows a DamID binding profile distinct from the other subtypes, suggesting a unique function. H1 subtypes can mark specific domains and repressive regions, pointing toward a role for H1 in three-dimensional genome organization. Our work integrates H1 subtypes into the epigenome maps of human cells and provides a valuable resource to refine our understanding of the significance of H1 and its heterogeneity in the control of genome function.

INTRODUCTION

The linker histone H1 is a key structural component of chromatin. It binds the DNA entering and exiting the nucleosome, sealing two turns of DNA around the histone octamers (Bednar et al., 1998; Thoma et al., 1979). Because of its capacity to promote and stabilize the folding of chromatin into higher-order structures in vitro, H1 might limit the access of transcription factors to DNA and thus has been proposed to act primarily as a transcriptional repressor (Schlissel and Brown, 1984). However, this model is difficult to reconcile with knockout studies in several organisms in which only a few changes in gene expression (including both up- and downregulation) occurred (Shen and Gorovsky, 1996; Takami et al., 2000; Fan et al., 2001; Alami et al., 2003). Moreover, it was recently demonstrated that in vitro, chromatin-containing H1 is not completely inaccessible and can still be remodeled by ATPase-containing complexes (Maier et al., 2008; Clausell et al., 2009).

An additional level of complexity is added by the existence of a variable number of closely related H1 proteins in higher eukaryotes, often referred to as subtypes (Izzo et al., 2008). In humans, 11 H1 subtypes with cell-type-specific and different temporal expression have been identified, including five canonical, replication-dependent somatic subtypes (H1.1–H1.5; for a review, see Happel and Doenecke, 2009). Despite their abundance and their potential specialization, gene ablation of individual somatic H1 subtypes in mice failed to reveal an essential role, leading to the assumption that H1 subtypes are redundant (Fan et al., 2001). However, inactivation of three somatic H1 subtypes in mice demonstrated that correct H1 levels are critical for proper development and that ~50% reduction of H1 is early-embryonic lethal (Fan et al., 2005). Moreover, several biochemical studies pointed toward more individual functions for H1 subtypes; for example, H1 subtypes differ in their capacity to compact nucleosomal arrays in vitro, and bind chromatin with different affinities in vivo (Liao and Cole, 1981; Talasz et al., 1998; Orrego et al., 2007; Clausell et al., 2009; Th'ng et al., 2005). Furthermore, H1 subtypes carry distinct posttranslational modifications and interact with different regulatory proteins (Wisniewski et al., 2007; Weiss et al., 2010; Lennox et al., 1982; Montes de Oca et al., 2005; Kamieniarz et al., 2012). Additionally, in microscopy and biochemical fractionation studies, individual subtypes showed discrete patterns of localization (Parseghian et al., 2000; Th'ng et al., 2005) and, importantly, displayed varied effects on gene regulation (Sancho et al., 2008; Gunjan and Brown, 1999; Bhan et al., 2008; Brown et al., 1996), arguing for H1-subtype-specific functions. Evolutionary analysis of the rates of nucleotide substitutions of H1 subtypes supports the notion of a functional differentiation of these subtypes (Ponte et al., 1998). Thus, it is possible that compensatory mechanisms activated to recapitulate a normal H1-to-nucleosome ratio could partially mask the functional importance of H1 heterogeneity. However, due to the lack of subtype-specific antibodies, the genomic distribution of H1 subtypes in vivo has not been addressed and the role of H1 subtypes in chromatin-related processes has thus far remained elusive.

The DNA adenine methyltransferase identification (DamID) technique is a method for identifying target sequences of chromatin-binding proteins. It is based on the expression of a protein of interest fused to Dam (van Steensel and Henikoff, 2000), a bacterial methyltransferase that specifically methylates adenines within GATC sequences (Greil et al., 2006). Because adenine methylation is absent in mammals, the methylation pattern can be used to infer the binding pattern of its fusion partner (van Steensel et al., 2001). DamID is now a well-established technology and has been used successfully to characterize the genomic binding of multiple chromatin components (Greil et al., 2006; Tolhuis et al., 2006; Nègre et al., 2006; Filion et al., 2010), including *Drosophila* H1 (Braunschweig et al., 2009). Based on this, we employed the DamID technique as an antibody-independent approach to systematically map the genomic distribution of all replication-dependent somatic H1 subtypes in human cells. Our analysis revealed DNA and chromatin features that potentially regulate the recruitment of H1 subtypes to chromatin. In particular CpG-dense regions and regulatory regions associated with active transcription seem to be devoid of H1. However, transcription alone is not sufficient to explain H1 recruitment to chromatin, and the presence of stably bound factors at both active and inactive regions might be critical for H1 binding. Moreover, our data indicate a possible role of somatic H1 subtypes in the three-dimensional organization of the genome within the cell nucleus. Finally, our data point toward a special role for the H1.1 subtype in chromatin function.

RESULTS

Histone H1 Subtypes Display a Similar Genomic Distribution with Dips at Promoters

In order to map the genomic distribution of the five canonical, replication-dependent linker histone H1 subtypes, we employed the DamID technique in human fibroblast IMR90 cells. We verified correct and comparable expression of H1 subtypes by RT-PCR and confirmed that fusion to Dam has no detectable effect on chromatin binding (Figures S1A and S1B; data not shown). Each data set was generated in duplicate under standardized conditions and H1 binding was detected by hybridization on NimbleGen oligonucleotide arrays. The data were normalized as described in the Materials and Methods section, and H1 binding is presented throughout this work as the $\log_2$ ratio of Dam-H1 fusion to Dam enzyme alone: $\log_2$(Dam-H1/Dam) (Braunschweig et al., 2009). A $\log_2$ ratio of zero can be interpreted as an average steady-state level of the given H1 subtype binding to chromatin, whereas negative and positive values correspond to a relative depletion and enrichment of the H1 subtype, respectively.

A comparison of the normalized DamID profiles showed an overall similar global distribution for the H1 subtypes H1.2–H1.5 (Figure S1C), with both dips and enrichments. According to our DamID data, H1.1 seems to have a different genomic localization compared with the other H1 subtypes. Using a simple running median-based algorithm, we identified specific regions that are either depleted or enriched for each H1 subtype in our data. The average size of the depleted and enriched regions was ~1,000 bp and 800 bp, respectively. Therefore, the H1-subtype enrichments identified are distinct and localized to particular genomic regions rather than to broad domains. Annotation of the identified regions to the human genome revealed a clear overrepresentation of depleted regions of all H1 subtypes at promoters (Figure 1A). In contrast to this, we found regions enriched for all H1 subtypes overrepresented at exons. Intergenic regions are preferentially bound by H1.2–H1.5, and a small fraction of H1.1-enriched regions correspond to promoters (Figure 1A). In addition to their similar distribution throughout the genome, a closer look at individual chromosomes in the DamID data revealed unique H1 subtype DamID patterns consisting of a combination of H1 subtypes with varying degrees of enrichment (Figure 1B). For example, chromosomes 14 and 15 are relatively depleted of H1, whereas chromosomes X, 18, and 20 show higher than average H1 binding (Figures 1B and S1D). Strikingly H1.2 appears enriched at chromosome X, with no preference for any particular DNA feature analyzed (Figures 1B, 1C, and S1E), and H1.1 on the highly transcriptionally active chromosome 19 (Figures 1B, 1C, and S1D).

In order to identify distinct combinations of H1 subtypes that are recurrent throughout the genome, we performed segmentation using an unbiased hidden Markov model (HMM) approach. We found that a five-state model optimally described our DamID data (see Materials and Methods). In this model, state 3 is the most abundant one, covering 50% of all probed locations, and corresponds to an average steady-state level of all five H1 subtypes binding (Figure 1D). State 1 corresponds to regions strongly depleted of all H1 subtypes in the DamID data sets, and shows 3.6% genome coverage. States 2, 4, and 5 show a similar level of H1.1 binding and different levels of H1.2–H1.5 enrichment. State 2, which covers 19.3% of the genome, and state 4, with 20.5% coverage, show a slight depletion and enrichment, respectively, of H1.2–H1.5. State 5, covering 6.2% of probed locations, corresponds to high enrichments of H1.2–H1.5 and highly variable H1.1 binding. The fact that none of the identified states distinguished between the subtypes H1.2–H1.5 supports the similarity of their distribution. We further corroborated this observation by independently calculating the correlation coefficients among our data sets for all somatic H1 subtypes. Indeed, the DamID results suggest the existence of two distinct groups: one consisting of H1.1 and one comprised of H1.2–H1.5 (Figure 1E). To gain insight into the molecular function of genes whose transcription start site (TSS) is found within these five HMM states, we performed a Gene Ontology (GO) analysis (Table S1). Genes within states 1 and 2 have a wide range of molecular functions and are only weakly enriched in a wide range of GO categories (e.g., DNA or protein binding), whereas genes within states 3–5 belong preferentially to fewer specialized categories.

H1 Subtypes Are Depleted at Active Promoters and Regulatory Elements

Linker histone H1 has been associated with transcriptional regulation both in vivo and in vitro (Alami et al., 2003; Bhan et al., 2008; Koop et al., 2003; Talasz et al., 1998). In order to investigate whether the depletion of H1 subtypes at promoters is linked to the transcriptional status of the corresponding genes, we divided

Cell PRESS
Open ACCESS

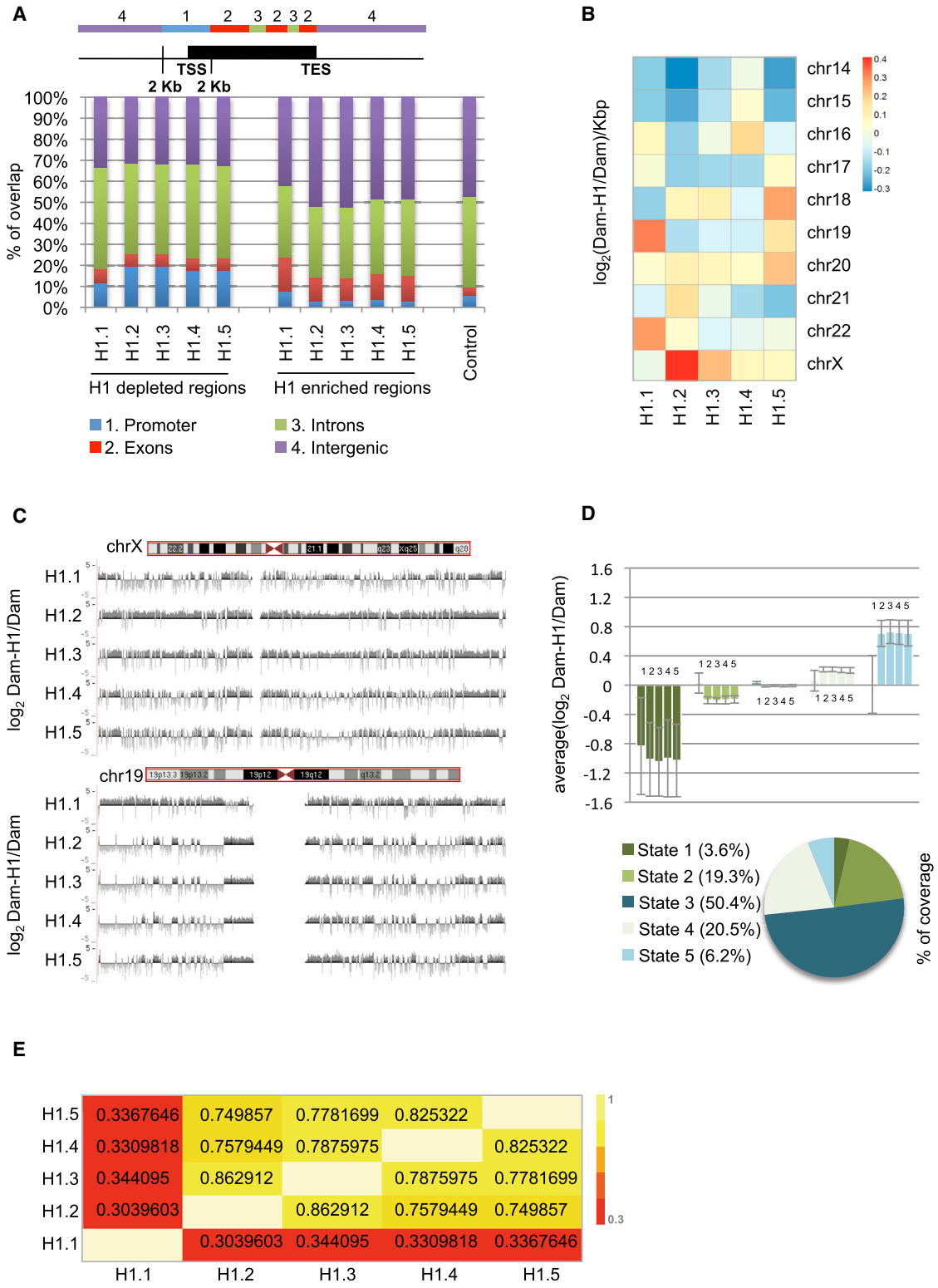

Figure 1. Genomic DamID Profile of Somatic H1 Subtypes

(A) Genomic annotation of regions found to be enriched and depleted of individual H1 subtypes. The length of the colored bars represents the percentage of regions enriched or depleted of H1 subtypes (as defined in Materials and Methods) overlapping with the indicated genomic features. As a control, the genomic annotation of all array probes is shown. Promoters are defined as RefGene TSSs flanked by 2 kb upstream and downstream. The genomic coordinates of exons

(legend continued on next page)

annotated human genes into four categories according to their expression level and analyzed the DamID binding values of H1 subtypes around the TSS. As shown in Figure 2A, H1 subtypes tend to be depleted from the TSS, and this depletion becomes more pronounced with increasing levels of gene expression. H1.1 shows the weakest tendency for this anticorrelation. Interestingly, in highly expressed genes, the H1 dips shift toward the gene body. This is in line with the differential positioning of the +1 nucleosome downstream from the TSS between active and silent genes (Schones et al., 2008). In addition to promoters, H1 subtypes also tend to be depleted from *cis*-regulatory regions such as enhancers and CTCF-bound insulators (Figure 2B), again with H1.1 being the least depleted subtype. In particular, active enhancers show the strongest depletion of H1, which is even higher than that of active promoters (compare Figures 2A and 2B). Furthermore, H1 is broadly distributed along the body of genes and at the 3′ UTR (Figure 2C) with more variable binding at exons as compared with introns. At the 5′ UTR, H1 is slightly depleted in comparison with the coding region, in agreement with different nucleosome densities at these regions, which are also characterized by lower DNA methylation levels (Choi, 2010).

Histone modifications can be considered as indicators of the transcriptional activity of promoters and other regulatory DNA elements (Kouzarides, 2007). We therefore analyzed the DamID binding values of H1 subtypes at regions enriched for several histone modifications. In line with our previous results, H1 subtypes seem to be depleted from chromatin marked by "active" histone modifications, such as H3K4me3 and H3K9ac, and inversely are slightly enriched at regions containing "repressive" histone modifications, such as H3K9me3 and H3K27me3 (Figure 2D). Interestingly, H1 does not seem to be depleted from H3K36me3-enriched regions that mainly mark exons of actively transcribed genes (Kolasinska-Zwierz et al., 2009).

CpG Islands Are Depleted of Histone H1 Subtypes

In human cells, 70% of promoters are associated with CpG islands and therefore can be classified according to their CG content (Saxonov et al., 2006). High-CpG promoters (HCPs) and low-CpG promoters (LCPs) represent strong CpG islands and clearly non-CpG islands, respectively. Intermediate-CpG promoters (ICPs) represent "weak" CpG islands (Weber et al., 2007). When we analyzed the DamID binding values of H1 at these promoter classes, we observed that the CG content negatively correlates with H1 binding values (Figures 3A and S2A). H1 subtypes tend to be depleted from HCPs (with the strongest depletion for H1.4 and the least depletion for H1.1), but not from LCPs, and an intermediate situation is present at ICP (Figures 3A and S2A). However, when they were sorted according to their expression level, it became evident that H1.2–H1.5 are mainly excluded from active and poised promoters regardless of their CG richness (Figure 3B). This inverse correlation between H1 binding values and transcription does not apply to all inactive promoters, since HCPs seem to remain H1-free even when repressed (Figure 3B). It has been shown that HCPs have a "permissive" chromatin structure and are bound by RNA-Polymerase II even when the gene they regulate is repressed (Guenther and Young, 2010). Therefore, it is possible that the presence of the transcription machinery, rather than the functional status of a promoter, is sufficient to displace H1.

Despite their frequent association with promoters, CpG islands can also be intragenic or intergenic (also called "orphan" CpG islands). With the exception of H1.1, H1 subtypes tend to be depleted from all types of CpG islands (Figure 3C). However, all H1 subtypes seem to be less depleted from inter- and intragenic-CpG islands as compared with promoter-CpG islands, and H1.1 is enriched at intragenic-CpG islands as compared with its average binding (Figure S2B). Overall, our results indicate that the degree of H1 displacement from CpG islands can be dependent on their genomic location.

The Distribution of Histone H1 Subtypes at DNA-Methylated Regions Is Context Dependent

So far, our data argue that gene expression correlates inversely with H1 binding. However, transcription per se is not sufficient to explain H1 distribution, since inactive HCPs tend to be devoid of H1 (Figure 3B) and CpG islands can be differentially bound by H1 subtypes (Figures 3C and S2B). Promoter-CpG islands are typically in an unmethylated state, whereas intra- and intergenic-CpG islands are more often found DNA methylated (Illingworth et al., 2010; Maunakea et al., 2010). We therefore analyzed the DamID binding values of H1 subtypes at CpG islands according to their density of methylation, and observed a positive correlation with DNA methylation (Figures 4A and S3A; Table S2). This tendency was consistent for all CpG island types independently of their location (data not shown). Although in most cases DNA methylation at promoter-CpG islands leads to gene silencing, this is not the case for orphan-CpG islands (Zilberman et al., 2007). Interestingly, intragenic-CpG islands are especially prone to DNA methylation (Illingworth et al., 2010; Maunakea et al., 2010), and this is well reflected by the slight enrichment of H1 subtypes (Figure S2B). As expected, we also found a positive correlation between H1 binding and DNA methylation at HCPs and ICPs (Figures 4B and S3B; Table S1). However, at LCPs, the presence of

and introns of RefSeq genes were retrieved from the UCSC Table Browser. Intergenic regions are defined as regions that do not overlap with promoters, exons, and introns.

(B) Distribution of H1 subtypes observed at individual chromosomes. The heatmap shows the H1 DamID binding values (log_2Dam-H1/Dam) per kilobase at individual chromosomes. Red color indicates enrichment, and blue color indicates depletion of the subtype.

(C) Distribution of H1 subtypes along chromosomes X and 19; DamID distribution viewed in the UCSC genome browser.

(D) H1 binding can be described by five principal states, each consisting of a unique combination of H1 subtypes. The bar graph shows the average DamID values (log_2Dam-H1/Dam) of H1 subtypes H1.1–H1.5 (1, 2, 3, 4, and 5) within each of the five HMM states. Error bars correspond to the SD. The pie chart shows the percentage of genome coverage of each of the five HMM states.

(E) Correlation of H1 subtypes genomic distribution. The heatmap shows the Pearson correlation coefficients calculated between H1 DamID binding values (log_2Dam-H1/Dam) across all probes on the array.

See also Figures S1 and S5 and Table S1.

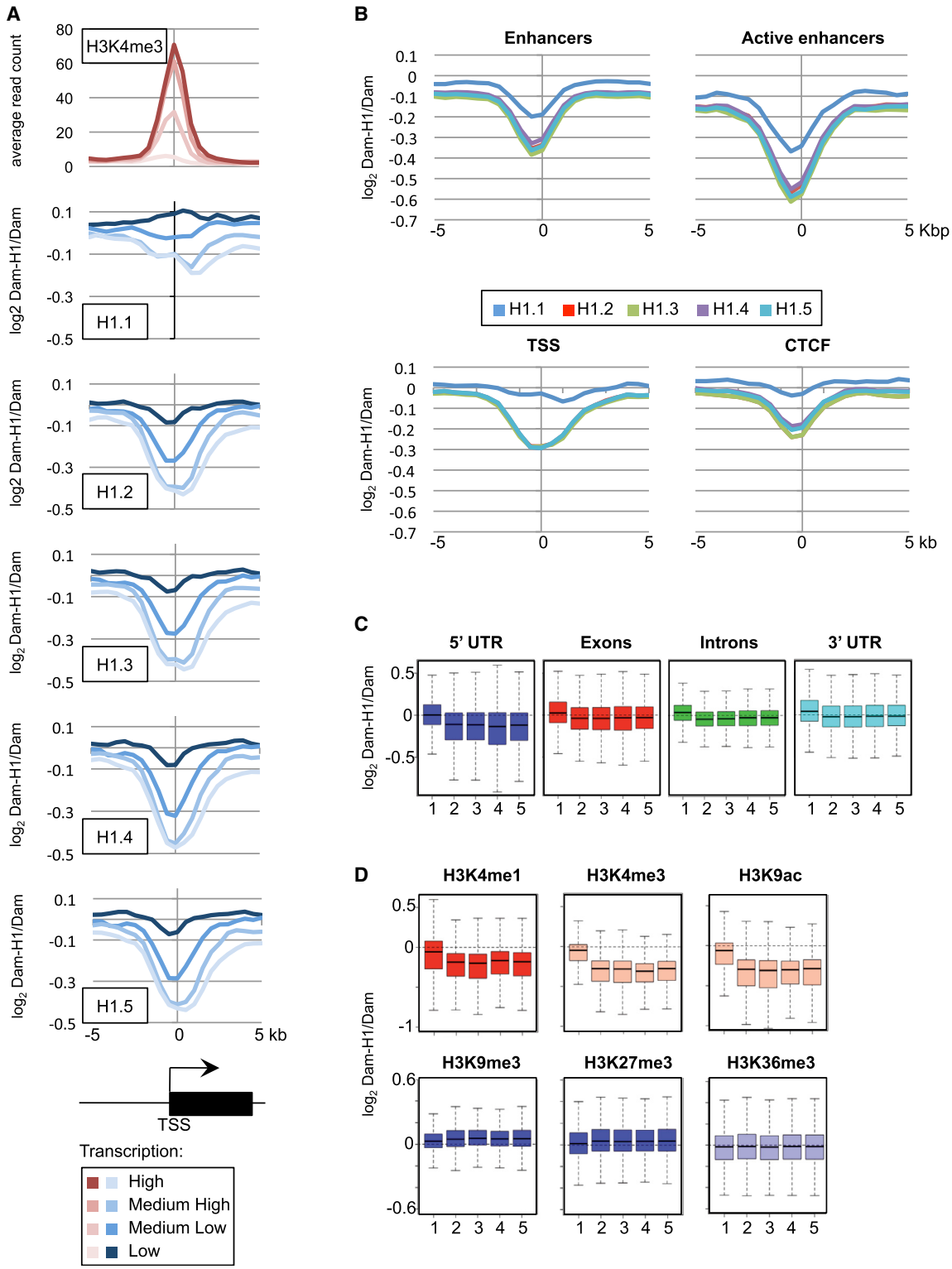

Figure 2. H1 Subtypes Are Depleted at Active TSS and Regulatory Regions

(A) H1 subtypes distribution observed around TSSs according to transcription levels. The averaged H1 DamID binding values (log_2Dam-H1/Dam) plotted 5 kb around the TSS of four categories of transcribed genes: highly transcribed (top 25%: high, light blue), medium highly transcribed (top middle 25%: medium high, medium light blue), medium lowly transcribed (bottom middle 25%: medium low, medium dark blue), and lowly/not transcribed (bottom 25%: low, dark blue). For comparison, the distribution of H3K4me3 reads around the TSS of the same transcribed genes is shown at the top.

(legend continued on next page)

H1.2–H1.5 seems to correlate negatively with DNA methylation (Figures 4B and S3B; Table S2). In contrast to HCPs and ICPs, LCPs do not show any significant correlation between gene activity and abundance of CpG methylation (Weber et al., 2007). Therefore, it is possible that a low density of methylation is not sufficient for effective repression of LCP-associated genes, and that the preferential presence of H1 at LCPs might contribute to their silencing.

In contrast to what we observed for CpG islands and HCPs, the binding values of H1 subtypes to gene bodies seems to correlate negatively with DNA methylation (Figures 4C and S3C; Table S2), and H1 subtypes bind preferentially at unmethylated gene bodies (Figure S3C). Interestingly H1.1 seems to be enriched at highly methylated exons and its binding values decrease proportionally with the levels of DNA methylation (Figure S3D). In contrast to this, H1.2–H1.5 subtypes tend to be depleted at highly methylated exons.

The Spatial Distribution of H1 Subtypes Is Indicative of Functionally Distinct Chromatin Domains

The recent development of novel powerful techniques has provided insights into the three-dimensional organization of the genome, demonstrating the existence of many transient contacts between genomic loci that are up to several megabases apart (Fullwood and Ruan, 2009; van Steensel, 2011). These regions of highly frequent intra- and intermolecular interactions have been defined as ''topological domains'' and the shorter chromatin segments separating them as ''topological boundaries'' (Dixon et al., 2012). Because of its long-studied structural role in local chromatin compaction, linker histone H1 is a good candidate for regulating the spatial organization of the genome within the nucleus. Recently, Dixon et al. (2012) employed the high-throughput chromosome conformation capture (Hi-C) method to map chromatin interactions in IMR90 cells. We therefore compared their data set with our DamID profiles. The DamID binding values of H1 subtypes show a very similar distribution at both domains and boundaries, with a median binding centered around zero (Figure 5A). The higher variance at boundaries could be explained by their smaller size (Figure S4A). This suggests that H1 might not be involved in demarcating topological boundaries versus domains at a global level. However, it was previously suggested that repressive domains are governed by an intrinsic folding regime that is significantly different from active chromatin regions (Sexton et al., 2012), and differential H1 binding could mediate those differences. To investigate this notion, we performed clustering of topological domains according to the enrichment of known epigenetic marks and chromatin regulators as previously described in *Drosophila* (Sexton et al., 2012). We analyzed four major classes of domains with clear biological functions for the enrichment/depletion of H1 subtypes: active domains (characterized by enrichment of H3K36me3 and H3K4me3), PcG domains (H3K27me3 enriched, mainly transcriptionally repressed), HP1 domains (H3K9me3 enriched, mainly transcriptionally repressed), and null domains (not enriched for any mark). Based on our DamID mapping, we find that different combinations of H1 subtypes can associate with functionally distinct topological domains: H1.1 seems to be preferentially enriched in PcG domains and slightly enriched in active domains, whereas H1.2–H1.5 are enriched in HP1 and null domains and depleted from active domains (Figure 5B).

An additional mechanism that contributes to the spatial organization of the genome is the anchoring of chromatin segments to the nuclear periphery by lamina-associated domains (LADs) (Guelen et al., 2008; Peric-Hupkes et al., 2010). Interestingly, we observed a strong enrichment of H1 within LADs (Figures 5C and 5D), and that changes in H1.2–H1.5 distribution can demarcate LAD boundaries (Figure S4B). In support of this observation, we found that depletion of H1.4 can globally affect the localization of lamins at the nuclear periphery (Figure S4C).

Although the precise molecular basis for this association of H1 with specific functional domains remains to be elucidated, these data suggest that distinct H1 subtypes have a preference for certain genomic regions and might be implicated in the formation of repressive chromatin domains, clearly distinguishing them from active chromatin.

DISCUSSION

Here, we present a comprehensive analysis of the genomic distribution of all somatic, replication-dependent human linker histone H1 subtypes. Because currently the specificity of H1 subtype-specific antibodies in ChIP assays is questionable, we employed an unbiased method, DamID.

DamID as a Method for Studying H1 Subtypes

DamID is now a well-established technique and often is the only valid alternative to chromatin immunoprecipitation (ChIP) in genome-wide studies. Due to the lack of linker histone H1 subtype-specific antibodies, DamID is a method of choice for analyzing the genomic distribution of H1 subtypes. In addition, DamID has a number of other important advantages. First, DamID detects protein-DNA interactions as they occur in living cells. Moreover, the Dam fusion protein is expressed at very

(B) Occupancy profile of H1 subtypes at regulatory elements. The averaged H1 DamID binding values are plotted 5 kb around the center of all putative enhancer regions, predicted active enhancers (as defined in Materials and Methods), the TSS of all (transcribed and not transcribed) annotated genes (according to UCSC refGene), and CTCF binding sites (Kim et al., 2007).

(C) H1 subtypes distribution observed within genes. Boxplots show the distribution of the H1 DamID binding values within the indicated regions. Here and in all figures the black line marks the median, and lower and upper limits of the box mark the first and third quartiles. Genomic coordinates of human 5′ UTRs, exons, introns, and 3′ UTRs were retrieved from the UCSC Table Browser. Numbers 1–5 indicate the corresponding H1 subtypes H1.1–H1.5.

(D) H1 subtypes distribution at regions enriched for the indicated histone modifications. The distribution of the H1 binding values is shown as a boxplot. Red and light red boxes indicate regions enriched for active histone modifications at enhancers (H3K4me1) and promoters (H3K4me3 and H3K9ac), respectively. Violet and light violet indicate repressive histone modifications (H3K9me3 and H3K27me3) and modifications at gene bodies (H3K36me3), respectively.

See also Figure S5.

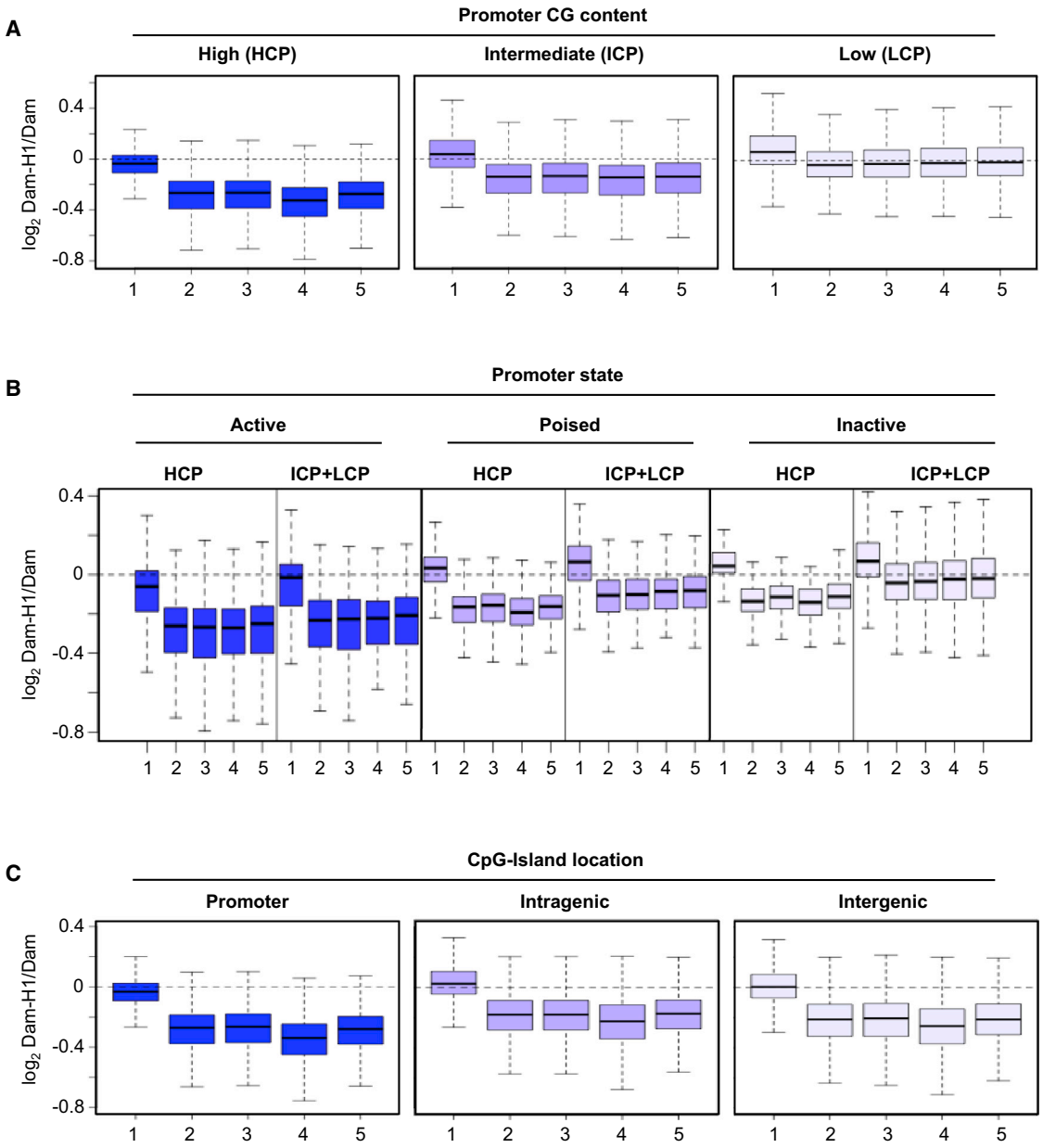

Figure 3. CpG-Rich Regions Are Depleted of H1 Subtypes

(A) H1 subtypes distribution at promoters with different CG content. Promoters have been classified into HCPs, ICPs, and LCPs according to Weber et al. (2007). The distribution of the H1 DamID binding values (log_2Dam-H1/Dam) in these promoter classes is shown as a boxplot. The dark to light violet color gradient indicates the levels of CG content from high to low.

(B) H1 subtypes distribution at promoter classes depending on their transcriptional state. Boxplots show the distribution of the H1 DamID binding values for each promoter class further subdivided into active, poised, and inactive promoters as defined in Materials and Methods. The dark to light violet color gradient corresponds to active, poised, and inactive transcriptional states of the indicated promoter.

(C) H1 subtype distributions at CpG islands. Boxplots show the distribution of the H1 DamID binding values at CpG islands associated with promoter-, intragenic-, and intergenic-CpG islands, defined as described in Materials and Methods.

See also Figures S2 and S5.

low levels and thus is unlikely to interfere with the functions of the endogenous protein or its targets. Third, DamID is a suitable method for proteins with relatively short residence times (Gelbart et al., 2005; Schmiedeberg et al., 2009; Misteli et al., 2000) because the adenine methylation remains after the protein has dissociated. Overall, detailed comparisons have extensively shown that DamID identifies the same binding sites and profiles as ChIP for a variety of proteins in different species (Greil et al., 2006; Tolhuis et al., 2006; Nègre et al., 2006; Filion et al., 2010). Importantly, the DamID binding profile

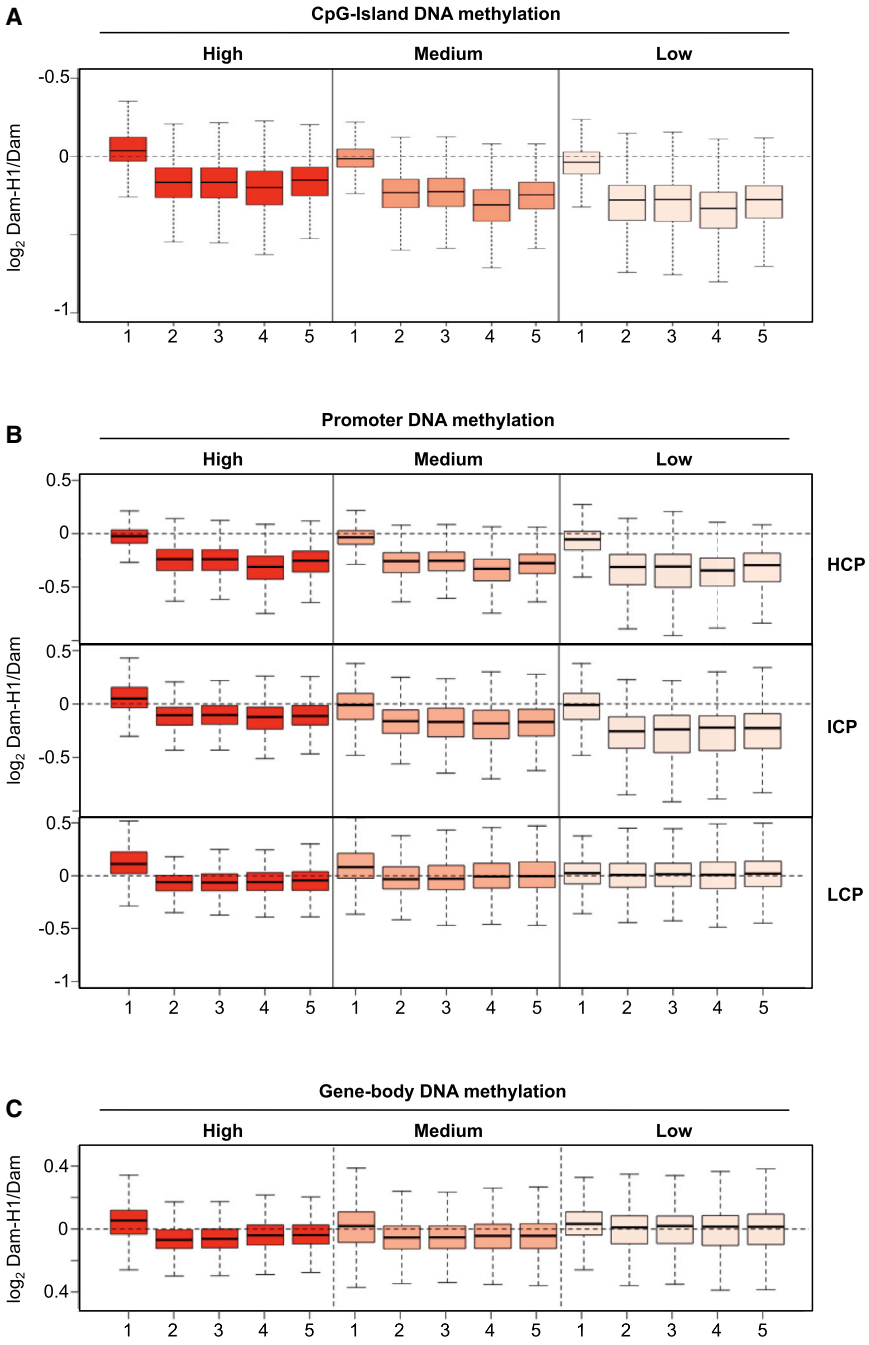

Figure 4. DNA Methylation Can Affect H1 Binding in a Context-Dependent Manner

(A) Observed H1 subtypes distribution at CpG islands according to their density of methylation. DNA methylation density was defined as the proportion of methylated cytosines per basepair. CpG islands were scored for DNA methylation as described in Materials and Methods and then divided into three groups of decreasing DNA methylation density (high, medium, low). The distribution of the H1 DamID binding values (log_2Dam-H1/Dam) is shown as a boxplot. The density of DNA methylation is color coded by decreasing intensities of red.

(B) H1 subtypes distribution at promoter classes according to their density of methylation. Boxplots show distribution of the H1 DamID binding values for HCP, ICP, and LCP classes, with each further divided into three groups of decreasing DNA methylation density as described in Materials and Methods. Red, light red, and rose boxes correspond to high, medium, and low density of DNA methylation, respectively.

(C) H1 subtypes distribution within gene bodies according to their density of methylation. DNA methylation density at the gene body, as defined in Materials and Methods, is scored as described for CpG islands, and the distributions of the H1 DamID binding values are shown as a boxplot. The levels of DNA methylation density are color coded as in (A) and (B).

See also Figures S3 and S5 and Table S2.

of *Drosophila* H1 (under conditions comparable to ours) has been directly compared twice with its genomic binding obtained by ChIP (Filion et al., 2010; Braunschweig et al., 2009), confirming that fusion to Dam does not alter the chromatin-binding properties of linker histone and that DamID is a valid method for studying H1 distribution. We also validated key features of the genomic distribution of H1 subtypes identified by DamID by quantitative ChIP-PCR in HEK293 stably expressing Flag-HA-H1.1 and Flag-HA-H1.4 (Figure S5), further strengthening our results.

However, the application of DamID has some potential limitations. It requires a relatively long time to express the fusion protein (Filion et al., 2010). However, this does not represent a limitation in our study, which focuses on unraveling the average chromatin-binding sites of linker histone H1 subtypes in a large population of unsynchronized cells. Furthermore, the DamID approach we used has a resolution of ~1 kb (Greil et al., 2006), which is comparable to the resolution of traditional ChIP with chromatin fragments of ~1 kb, but is 2–3 times lower than that achieved by recent ChIP-sequencing approaches. Although such resolution may not always be sufficient to determine the accurate binding position of every protein on a single-locus level, an average binding profile in a metagene-type analysis, such as the one obtained in our study, is highly informative and robust.

Genomic Distribution of H1 Subtypes

In our analysis, we found that globally human H1 subtypes (H1.2–H1.5) tend to have a very similar distribution, with both specific dips and enrichments. Although the enrichments/depletions we observe are relatively slight, we expect them to be biologically relevant, since a similar situation of small but functionally

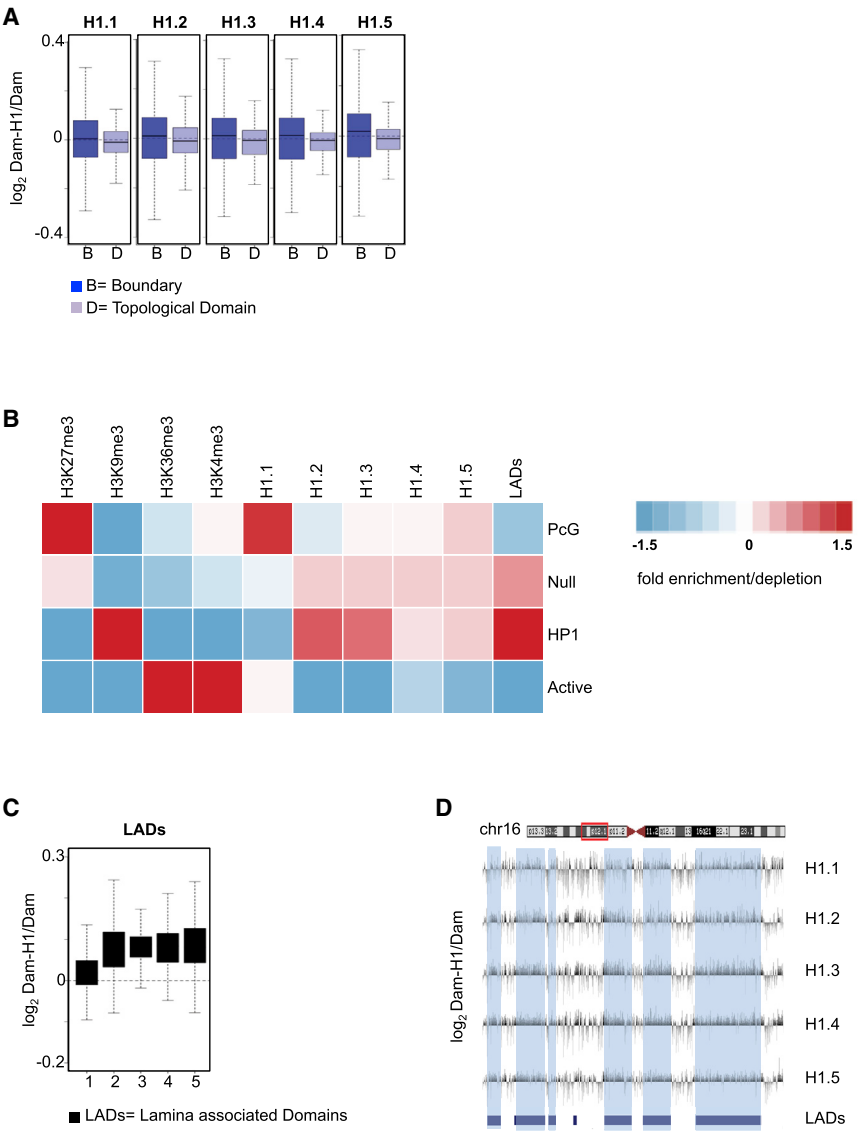

Figure 5. The Spatial Distribution of H1 Subtypes in the Nucleus Overlaps with Repressive Chromatin Domains

(A) H1 subtypes distribution at topological domains versus boundaries. Boxplots show the distribution of H1 DamID binding values (log_2Dam-H1/Dam) within the topological domains and their boundaries, as defined using Hi-C in human IMR90 cells (Dixon et al., 2012). Violet boxes represent boundaries and light violet boxes indicate domains.

(B) H1 subtypes enrichment at topological domains assigned to four epigenetic classes. Heatmap shows enrichment (red) and depletion (blue) with respect to random expectations of specific histone marks, H1.1–H1.5, and LADs within each of four epigenetic classes of physical domains determined by Hi-C (Dixon et al., 2012) and defined according to Sexton et al. (2012). The epigenetic marks used for supervised clustering into polycomb (PcG), HP1, active, and null domains were H3K27me3, H3K9me3, H3K36me3, and H3K4me3, respectively.

(C and D) H1 subtypes enrichment at LADs.

(C) Black boxplots show the distributions of the H1 DamID binding values (log_2Dam-H1/Dam) within LADs, as previously defined (Guelen et al., 2008).

(D) Genome browser snapshot of the H1 subtypes distribution at a subregion of chr16 (red box). The position of LADs is indicated by blue boxes at the bottom of H1 DamID profiles, and the highlighted light blue regions show the H1 distribution within LADs.

See also Figures S4 and S5.

important enrichments on regulatory elements has also been reported for the core histone variant H3.3 (Goldberg et al., 2010).

In general, we found H1 subtypes to be depleted from active promoters as well as from regulatory elements controlling transcription, and enriched at regions carrying repressive histone marks such as H3K9me3 and H3K27me3. In particular, CpG-dense regions often seem to be devoid of H1.2–H1.5. We found that the depletion of H1 subtypes is generally less pronounced at intra- and intergenic (orphan) CpG islands than at promoter-CpG islands. Based on this, we speculate that CpG islands are differently bound by H1 depending on their location. Many orphan-CpG islands represent alternative promoters of annotated genes, whereas others are initiation sites of noncoding RNA transcription (Illingworth et al., 2010), suggesting that active transcription might trigger the loss of H1 at CpG-dense regions. Furthermore, we found that H1 subtypes are present within gene bodies, with less pronounced changes depending on the transcription levels (data not shown). This suggests that H1 binding might be more sensitive to initiation of transcription than to transcriptional elongation. This is in line with previous findings that other chromatin marks, such as DNA methylation and the methyl-CpG binding protein 2 (MeCP2), are associated with silencing when present at the TSS but are permissive for transcription when found within gene bodies (Jones, 1999).

Transcription does not seem to be the only determinant of the genomic distribution of H1, since, e.g., poised promoters and inactive HCPs can also be depleted of H1. A recent analysis indicated that promoter-CpG islands are kept in a nucleosome-free state through the stable binding of regulatory factors (Choi, 2010). Thus, H1 distribution might also be regulated by other chromatin proteins rather than simply being a consequence of transcription or an intrinsic limitation of H1 binding to CG-rich DNA. We therefore favor a model in which H1 binding is regulated at multiple levels and H1 subtypes act as fine-tuners of gene regulation.

The Link between DNA Methylation and H1 Binding

The functional link between DNA methylation and H1 binding has been under discussion for a long time, and partially contradictory

results regarding the preferential recruitment of H1 on methylated versus unmethylated chromatin have been reported (Nightingale and Wolffe, 1995; McArthur and Thomas, 1996; Ball et al., 1983; Campoy et al., 1995). There could be several reasons for these apparent discrepancies. In early in vitro experiments, investigators used total H1 purified from different sources without considering the variation in the relative amount of H1 subtypes (Helliger et al., 1992; Lennox and Cohen, 1983). Furthermore, the affinity of H1 subtypes for methylated DNA was often measured in vitro on naked DNA instead of nucleosomes (Strom et al., 1995; McArthur and Thomas, 1996). Purified H1 subtypes might also lack their original modifications, which are known to have important consequences for gene regulation (Kamieniarz et al., 2012; Weiss et al., 2010; Hergeth et al., 2011). Our data show that on a genomic scale in vivo, there seems to be no simple correlation between H1 binding and DNA methylation, and instead the presence of H1 at methylated regions could be dependent on the genomic location and therefore on the chromatin context.

Role of H1 in Higher Order of Chromatin Structure

It has now became evident that chromatin is organized within the nucleus according to specific biological functions (Duan and Blau, 2012). Three main molecular mechanisms have been proposed to explain how chromatin can acquire its three-dimensional configuration: (1) local chromatin compaction into irregular patches of aggregated nucleosomes, (2) inter- and intramolecular interactions between distant DNA elements into topological domains, and (3) anchoring of chromatin to nuclear scaffolds (van Steensel, 2011). Because of its ability to regulate chromatin compaction, it has been suggested that H1 could play a key role in the spatial organization of the genome. However, this interesting possibility has not been addressed thus far. Our mapping data and the analysis of H1 distribution within topological domains suggest that differences among H1 subtypes at the linear genomic level can be recapitulated within the tridimensional organization of nuclear space. In particular, H1 subtypes could take part in the global segmentation of the genome into active and inactive regions (domains) and be implicated in the establishment and/or maintenance of LADs. This suggestion is in agreement with previous findings that LADs contain mainly transcriptionally silent genes (Guelen et al., 2008) and are mainly associated with HP1 and null domains, similarly to H1.2–H1.5 (Figure 5B). Moreover, the insulator protein CTCF and CpG islands can delimit the borders of LADs (Guelen et al., 2008), regions we have found to be depleted of H1. In line with this, changes in H1.2–H1.5 distribution can demarcate LAD boundaries. Together, these results suggest a possible involvement of H1 in LAD confinement.

It has been proposed that in addition to gene regulation, attachment of genomic regions to the nuclear lamina contributes to the spatial organization of interphase chromosomes inside the nucleus (Guelen et al., 2008). In line with this, we noticed that different combinations of H1 subtypes can be enriched at individual chromosomes, and in particular chromosomes with the highest LAD coverage also have the strongest H1.2–H1.5 enrichment (Figures 1B and S1D). This specific H1 pattern might contribute to the compartmentalization of chromosomes into specific territories (Cremer and Cremer, 2001) through, e.g., direct local chromatin compaction, which could be dependent on the H1 subtypes present and/or the recruitment of H1 subtype-specific interactors, which in turn could tether H1-bound regions to different nuclear locations.

H1.1 Is a Special H1 Subtype

Our analysis suggests that, based on their DamID binding values, H1 subtypes can be divided into two groups: (1) H1.1 and (2) H1.2–H1.5. We found that the differences between the enrichment of H1.1 and that of H1.2–H1.5 seem to be more pronounced at regulatory regions marked by activating histone modifications such as promoters, enhancers, and CpG islands (Figures 2 and 3). For example, we observed in our DamID profiling that although H1.1 is not depleted at inactive and poised HCPs, H1.2–H1.5 are (Figure 3B). HCPs are often associated with developmentally regulated genes (Zhu et al., 2008), which need to be activated in response to external stimuli and therefore do not require a stable repressive chromatin organization. Moreover, although CG richness can affect H1 subtype binding to chromatin similarly (Figure S3A), H1.1 is the only subtype that displays a rather positive correlation with DNA methylation independently of its genomic location (Figure S3B; Table S2).

Based on these findings, we propose that H1.1 is somehow special among H1 subtypes. The chromatin structure promoted by H1.1 binding might support a level of compaction that facilitates rapid conversion into either an active or repressed state. Previous data also agree with this special role for H1.1. For example, it was shown that H1.1 had the least ability to condense nucleosomes in vitro (Khadake and Rao, 1995), and had the lowest affinity to chromatin both in fluorescence recovery after photobleaching experiments in vivo and biochemical studies in vitro (Orrego et al., 2007; Th'ng et al., 2005). The dynamic binding of H1.1 might at least in part explain why chromatin-containing H1.1 does not necessarily impede gene expression. In line with this, Alami et al. (2003) showed that H1.1 has a unique role in activating a reporter transgene in mice. In view of its distinct distribution and its potential association with more active and open chromatin, it is not surprising that H1.1 expression is restricted to certain cells, thereby conferring some tissue-specific function (Piña et al., 1987). Interestingly, estimation of the degree of nucleotide substitutions during evolution also pointed toward a functional differentiation of H1.1 from the other H1 subtypes, further strengthening the uniqueness of H1.1 among the somatic H1 subtypes from an evolutionary perspective (Ponte et al., 1998).

In conclusion, we present here a genome-wide distribution of human linker histone H1 subtypes. Our comprehensive analysis represents a key step toward answering many open questions about the function of H1 and the significance of H1 heterogeneity in higher eukaryotes. Our work will also provide a resource for further studies to elucidate the molecular mechanisms that regulate H1 binding to chromatin, and the consequences of the functional diversity of H1 subtypes.

EXPERIMENTAL PROCEDURES

The DamID experiments were performed in IMR90 cells as previously described (Moorman et al., 2006). Normalization and analyses of DamID

data were performed using custom R scripts (http://www.r-project.org/), GenPlay software (Lajugie and Bouhassira, 2011), and Galaxy (Blankenberg et al., 2010). For more details, see Extended Experimental Procedures. Coordinates for the human RefSeq genes, introns, exons, 5′ UTRs, 3′ UTRs, CpG islands, and LADs were retrieved from the UCSC Table Browser. Histone-modification maps, gene-expression data, and bisulfite sequencing data for IMR90 cells were obtained from the Gene Expression Omnibus (GEO; data set GSE16256). The CTCF map for IMR90 cells was retrieved from GEO (data set GSE5559). Table S1 summarizes the Gene Ontology (GO) analysis of genes present in the HMM states. Table S2 shows the correlations of H1 binding and DNA methylation, and Table S3 includes the list of primers used in this study.

ACCESSION NUMBERS

The data have been submitted to the NCBI GEO under accession number GSE40886.

SUPPLEMENTAL INFORMATION

Supplemental Information includes Extended Experimental Procedures, five figures, and three tables and can be found with this article online at http://dx.doi.org/10.1016/j.celrep.2013.05.003.

LICENSING INFORMATION

ACKNOWLEDGMENTS

We thank Ulrich Braunschweig, Nicolas Fourel, and Nicolas Delhomme for valuable computational advice and members of R.S.'s laboratory for helpful discussions. Work in R.S.'s laboratory is supported by the DFG (through SFB 746), an ERC starting grant, and the FRM (Équipe Labilise). J.K. is supported by EMBO LTF and NWO-ALW VENI. B.v.S. is supported by NWO-ALW VICI.

Received: October 15, 2012
Revised: February 19, 2013
Accepted: May 3, 2013
Published: June 6, 2013

REFERENCES

Alami, R., Fan, Y., Pack, S., Sonbuchner, T.M., Besse, A., Lin, Q., Greally, J.M., Skoultchi, A.I., and Bouhassira, E.E. (2003). Mammalian linker-histone subtypes differentially affect gene expression in vivo. Proc. Natl. Acad. Sci. USA *100*, 5920–5925.

Ball, D.J., Gross, D.S., and Garrard, W.T. (1983). 5-methylcytosine is localized in nucleosomes that contain histone H1. Proc. Natl. Acad. Sci. USA *80*, 5490–5494.

Bednar, J., Horowitz, R.A., Grigoryev, S.A., Carruthers, L.M., Hansen, J.C., Koster, A.J., and Woodcock, C.L. (1998). Nucleosomes, linker DNA, and linker histone form a unique structural motif that directs the higher-order folding and compaction of chromatin. Proc. Natl. Acad. Sci. USA *95*, 14173–14178.

Bhan, S., May, W., Warren, S.L., and Sittman, D.B. (2008). Global gene expression analysis reveals specific and redundant roles for H1 variants, H1c and H1(0), in gene expression regulation. Gene *414*, 10–18.

Blankenberg, D., Von Kuster, G., Coraor, N., Ananda, G., Lazarus, R., Mangan, M., Nekrutenko, A., and Taylor, J. (2010). Galaxy: a web-based genome analysis tool for experimentalists. Curr. Protoc. Mol. Biol. *Chapter 19*, Unit 19.10.1–21.

Braunschweig, U., Hogan, G.J., Pagie, L., and van Steensel, B. (2009). Histone H1 binding is inhibited by histone variant H3.3. EMBO J. *28*, 3635–3645.

Brown, D.T., Alexander, B.T., and Sittman, D.B. (1996). Differential effect of H1 variant overexpression on cell cycle progression and gene expression. Nucleic Acids Res. *24*, 486–493.

Campoy, F.J., Meehan, R.R., McKay, S., Nixon, J., and Bird, A. (1995). Binding of histone H1 to DNA is indifferent to methylation at CpG sequences. J. Biol. Chem. *270*, 26473–26481.

Choi, J.K. (2010). Contrasting chromatin organization of CpG islands and exons in the human genome. Genome Biol. *11*, R70.

Clausell, J., Happel, N., Hale, T.K., Doenecke, D., and Beato, M. (2009). Histone H1 subtypes differentially modulate chromatin condensation without preventing ATP-dependent remodeling by SWI/SNF or NURF. PLoS ONE *4*, e0007243.

Cremer, T., and Cremer, C. (2001). Chromosome territories, nuclear architecture and gene regulation in mammalian cells. Nat. Rev. Genet. *2*, 292–301.

Dixon, J.R., Selvaraj, S., Yue, F., Kim, A., Li, Y., Shen, Y., Hu, M., Liu, J.S., and Ren, B. (2012). Topological domains in mammalian genomes identified by analysis of chromatin interactions. Nature *485*, 376–380.

Duan, Z., and Blau, C.A. (2012). The genome in space and time: does form always follow function? How does the spatial and temporal organization of a eukaryotic genome reflect and influence its functions? Bioessays *34*, 800–810.

Fan, Y., Sirotkin, A., Russell, R.G., Ayala, J., and Skoultchi, A.I. (2001). Individual somatic H1 subtypes are dispensable for mouse development even in mice lacking the H1(0) replacement subtype. Mol. Cell. Biol. *21*, 7933–7943.

Fan, Y., Nikitina, T., Zhao, J., Fleury, T.J., Bhattacharyya, R., Bouhassira, E.E., Stein, A., Woodcock, C.L., and Skoultchi, A.I. (2005). Histone H1 depletion in mammals alters global chromatin structure but causes specific changes in gene regulation. Cell *123*, 1199–1212.

Filion, G.J., van Bemmel, J.G., Braunschweig, U., Talhout, W., Kind, J., Ward, L.D., Brugman, W., de Castro, I.J., Kerkhoven, R.M., Bussemaker, H.J., et al. (2010). Systematic protein location mapping reveals five principal chromatin types in Drosophila cells. Cell *143*, 212–224.

Fullwood, M.J., and Ruan, Y. (2009). ChIP-based methods for the identification of long-range chromatin interactions. J. Cell. Biochem. *107*, 30–39.

Gelbart, M.E., Bachman, N., Delrow, J., Boeke, J.D., and Tsukiyama, T. (2005). Genome-wide identification of Isw2 chromatin-remodeling targets by localization of a catalytically inactive mutant. Genes Dev. *19*, 942–954.

Goldberg, A.D., Banaszynski, L.A., Noh, K.M., Lewis, P.W., Elsaesser, S.J., Stadler, S., Dewell, S., Law, M., Guo, X., Li, X., et al. (2010). Distinct factors control histone variant H3.3 localization at specific genomic regions. Cell *140*, 678–691.

Greil, F., Moorman, C., and van Steensel, B. (2006). DamID: mapping of in vivo protein-genome interactions using tethered DNA adenine methyltransferase. Methods Enzymol. *410*, 342–359.

Guelen, L., Pagie, L., Brasset, E., Meuleman, W., Faza, M.B., Talhout, W., Eussen, B.H., de Klein, A., Wessels, L., de Laat, W., et al. (2008). Domain organization of human chromosomes revealed by mapping of nuclear lamina interactions. Nature *453*, 948–951.

Guenther, M.G., and Young, R.A. (2010). Transcription. Repressive transcription. Science *329*, 150–151.

Gunjan, A., and Brown, D.T. (1999). Overproduction of histone H1 variants in vivo increases basal and induced activity of the mouse mammary tumor virus promoter. Nucleic Acids Res. *27*, 3355–3363.

Happel, N., and Doenecke, D. (2009). Histone H1 and its isoforms: contribution to chromatin structure and function. Gene *431*, 1–12.

Helliger, W., Lindner, H., Grübl-Knosp, O., and Puschendorf, B. (1992). Alteration in proportions of histone H1 variants during the differentiation of murine erythroleukaemic cells. Biochem. J. *288*, 747–751.

Hergeth, S.P., Dundr, M., Tropberger, P., Zee, B.M., Garcia, B.A., Daujat, S., and Schneider, R. (2011). Isoform-specific phosphorylation of human linker histone H1.4 in mitosis by the kinase Aurora B. J. Cell Sci. *124*, 1623–1628.

Illingworth, R.S., Gruenewald-Schneider, U., Webb, S., Kerr, A.R., James, K.D., Turner, D.J., Smith, C., Harrison, D.J., Andrews, R., and Bird, A.P. (2010). Orphan CpG islands identify numerous conserved promoters in the mammalian genome. PLoS Genet. *6*, 6.

Izzo, A., Kamieniarz, K., and Schneider, R. (2008). The histone H1 family: specific members, specific functions? Biol. Chem. *389*, 333–343.

Jones, P.A. (1999). The DNA methylation paradox. Trends Genet. *15*, 34–37.

Kamieniarz, K., Izzo, A., Dundr, M., Tropberger, P., Ozretic, L., Kirfel, J., Scheer, E., Tropel, P., Wisniewski, J.R., Tora, L., et al. (2012). A dual role of linker histone H1.4 Lys 34 acetylation in transcriptional activation. Genes Dev. *26*, 797–802.

Khadake, J.R., and Rao, M.R. (1995). DNA- and chromatin-condensing properties of rat testes H1a and H1t compared to those of rat liver H1bdec; H1t is a poor condenser of chromatin. Biochemistry *34*, 15792–15801.

Kim, T.H., Abdullaev, Z.K., Smith, A.D., Ching, K.A., Loukinov, D.I., Green, R.D., Zhang, M.Q., Lobanenkov, V.V., and Ren, B. (2007). Analysis of the vertebrate insulator protein CTCF-binding sites in the human genome. Cell *128*, 1231–1245.

Kolasinska-Zwierz, P., Down, T., Latorre, I., Liu, T., Liu, X.S., and Ahringer, J. (2009). Differential chromatin marking of introns and expressed exons by H3K36me3. Nat. Genet. *41*, 376–381.

Koop, R., Di Croce, L., and Beato, M. (2003). Histone H1 enhances synergistic activation of the MMTV promoter in chromatin. EMBO J. *22*, 588–599.

Kouzarides, T. (2007). Chromatin modifications and their function. Cell *128*, 693–705.

Lajugie, J., and Bouhassira, E.E. (2011). GenPlay, a multipurpose genome analyzer and browser. Bioinformatics *27*, 1889–1893.

Lennox, R.W., and Cohen, L.H. (1983). The histone H1 complements of dividing and nondividing cells of the mouse. J. Biol. Chem. *258*, 262–268.

Lennox, R.W., Oshima, R.G., and Cohen, L.H. (1982). The H1 histones and their interphase phosphorylated states in differentiated and undifferentiated cell lines derived from murine teratocarcinomas. J. Biol. Chem. *257*, 5183–5189.

Liao, L.W., and Cole, R.D. (1981). Differences among subfractions of H1 histone in their interactions with linear and superhelical DNA. Circular dichroism. J. Biol. Chem. *256*, 6751–6755.

Maier, V.K., Chioda, M., Rhodes, D., and Becker, P.B. (2008). ACF catalyses chromatosome movements in chromatin fibres. EMBO J. *27*, 817–826.

Maunakea, A.K., Nagarajan, R.P., Bilenky, M., Ballinger, T.J., D'Souza, C., Fouse, S.D., Johnson, B.E., Hong, C., Nielsen, C., Zhao, Y., et al. (2010). Conserved role of intragenic DNA methylation in regulating alternative promoters. Nature *466*, 253–257.

McArthur, M., and Thomas, J.O. (1996). A preference of histone H1 for methylated DNA. EMBO J. *15*, 1705–1714.

Misteli, T., Gunjan, A., Hock, R., Bustin, M., and Brown, D.T. (2000). Dynamic binding of histone H1 to chromatin in living cells. Nature *408*, 877–881.

Montes de Oca, R., Lee, K.K., and Wilson, K.L. (2005). Binding of barrier to autointegration factor (BAF) to histone H3 and selected linker histones including H1.1. J. Biol. Chem. *280*, 42252–42262.

Moorman, C., Sun, L.V., Wang, J., de Wit, E., Talhout, W., Ward, L.D., Greil, F., Lu, X.J., White, K.P., Bussemaker, H.J., and van Steensel, B. (2006). Hotspots of transcription factor colocalization in the genome of Drosophila melanogaster. Proc. Natl. Acad. Sci. USA *103*, 12027–12032.

Nègre, N., Hennetin, J., Sun, L.V., Lavrov, S., Bellis, M., White, K.P., and Cavalli, G. (2006). Chromosomal distribution of PcG proteins during Drosophila development. PLoS Biol. *4*, e170.

Nightingale, K., and Wolffe, A.P. (1995). Methylation at CpG sequences does not influence histone H1 binding to a nucleosome including a Xenopus borealis 5 S rRNA gene. J. Biol. Chem. *270*, 4197–4200.

Orrego, M., Ponte, I., Roque, A., Buschati, N., Mora, X., and Suau, P. (2007). Differential affinity of mammalian histone H1 somatic subtypes for DNA and chromatin. BMC Biol. *5*, 22.

Parseghian, M.H., Newcomb, R.L., Winokur, S.T., and Hamkalo, B.A. (2000). The distribution of somatic H1 subtypes is non-random on active vs. inactive chromatin: distribution in human fetal fibroblasts. Chromosome Res. *8*, 405–424.

Peric-Hupkes, D., Meuleman, W., Pagie, L., Bruggeman, S.W., Solovei, I., Brugman, W., Gräf, S., Flicek, P., Kerkhoven, R.M., van Lohuizen, M., et al. (2010). Molecular maps of the reorganization of genome-nuclear lamina interactions during differentiation. Mol. Cell *38*, 603–613.

Piña, B., Martínez, P., and Suau, P. (1987). Changes in H1 complement in differentiating rat-brain cortical neurons. Eur. J. Biochem. *164*, 71–76.

Ponte, I., Vidal-Taboada, J.M., and Suau, P. (1998). Evolution of the vertebrate H1 histone class: evidence for the functional differentiation of the subtypes. Mol. Biol. Evol. *15*, 702–708.

Sancho, M., Diani, E., Beato, M., and Jordan, A. (2008). Depletion of human histone H1 variants uncovers specific roles in gene expression and cell growth. PLoS Genet. *4*, e1000227.

Saxonov, S., Berg, P., and Brutlag, D.L. (2006). A genome-wide analysis of CpG dinucleotides in the human genome distinguishes two distinct classes of promoters. Proc. Natl. Acad. Sci. USA *103*, 1412–1417.

Schlissel, M.S., and Brown, D.D. (1984). The transcriptional regulation of Xenopus 5s RNA genes in chromatin: the roles of active stable transcription complexes and histone H1. Cell *37*, 903–913.

Schmiedeberg, L., Skene, P., Deaton, A., and Bird, A. (2009). A temporal threshold for formaldehyde crosslinking and fixation. PLoS ONE *4*, e4636.

Schones, D.E., Cui, K., Cuddapah, S., Roh, T.Y., Barski, A., Wang, Z., Wei, G., and Zhao, K. (2008). Dynamic regulation of nucleosome positioning in the human genome. Cell *132*, 887–898.

Sexton, T., Yaffe, E., Kenigsberg, E., Bantignies, F., Leblanc, B., Hoichman, M., Parrinello, H., Tanay, A., and Cavalli, G. (2012). Three-dimensional folding and functional organization principles of the Drosophila genome. Cell *148*, 458–472.

Shen, X., and Gorovsky, M.A. (1996). Linker histone H1 regulates specific gene expression but not global transcription in vivo. Cell *86*, 475–483.

Strom, R., Santoro, R., D'Erme, M., Mastrantonio, S., Reale, A., Marenzi, S., Zardo, G., and Caiafa, P. (1995). Specific variants of H1 histone regulate CpG methylation in eukaryotic DNA. Gene *157*, 253–256.

Takami, Y., Nishi, R., and Nakayama, T. (2000). Histone H1 variants play individual roles in transcription regulation in the DT40 chicken B cell line. Biochem. Biophys. Res. Commun. *268*, 501–508.

Talasz, H., Sapojnikova, N., Helliger, W., Lindner, H., and Puschendorf, B. (1998). In vitro binding of H1 histone subtypes to nucleosomal organized mouse mammary tumor virus long terminal repeat promotor. J. Biol. Chem. *273*, 32236–32243.

Th'ng, J.P., Sung, R., Ye, M., and Hendzel, M.J. (2005). H1 family histones in the nucleus. Control of binding and localization by the C-terminal domain. J. Biol. Chem. *280*, 27809–27814.

Thoma, F., Koller, T., and Klug, A. (1979). Involvement of histone H1 in the organization of the nucleosome and of the salt-dependent superstructures of chromatin. J. Cell Biol. *83*, 403–427.

Tolhuis, B., de Wit, E., Muijrers, I., Teunissen, H., Talhout, W., van Steensel, B., and van Lohuizen, M. (2006). Genome-wide profiling of PRC1 and PRC2 Polycomb chromatin binding in Drosophila melanogaster. Nat. Genet. *38*, 694–699.

van Steensel, B. (2011). Chromatin: constructing the big picture. EMBO J. *30*, 1885–1895.

van Steensel, B., and Henikoff, S. (2000). Identification of in vivo DNA targets of chromatin proteins using tethered dam methyltransferase. Nat. Biotechnol. *18*, 424–428.

van Steensel, B., Delrow, J., and Henikoff, S. (2001). Chromatin profiling using targeted DNA adenine methyltransferase. Nat. Genet. *27*, 304–308.

Weber, M., Hellmann, I., Stadler, M.B., Ramos, L., Pääbo, S., Rebhan, M., and Schübeler, D. (2007). Distribution, silencing potential and evolutionary impact of promoter DNA methylation in the human genome. Nat. Genet. *39*, 457–466.

Weiss, T., Hergeth, S., Zeissler, U., Izzo, A., Tropberger, P., Zee, B.M., Dundr, M., Garcia, B.A., Daujat, S., and Schneider, R. (2010). Histone H1 variant-specific lysine methylation by G9a/KMT1C and Glp1/KMT1D. Epigenetics Chromatin *3*, 7.

Wisniewski, J.R., Zougman, A., Krüger, S., and Mann, M. (2007). Mass spectrometric mapping of linker histone H1 variants reveals multiple acetylations, methylations, and phosphorylation as well as differences between cell culture and tissue. Mol. Cell. Proteomics *6*, 72–87.

Zhu, J., He, F., Hu, S., and Yu, J. (2008). On the nature of human housekeeping genes. Trends Genet. *24*, 481–484.

Zilberman, D., Gehring, M., Tran, R.K., Ballinger, T., and Henikoff, S. (2007). Genome-wide analysis of Arabidopsis thaliana DNA methylation uncovers an interdependence between methylation and transcription. Nat. Genet. *39*, 61–69.